

Controlled molecule injector for cold, dense, and pure molecular beams at the European x-ray free-electron laser

Lanhai He,^{1,2} Melby Johny,^{1,3,4} Thomas Kierspel,^{1,3,4} Karol Długołęcki,¹ Sadia Bari,⁵ Rebecca Boll,⁶ Hubertus Bromberger,¹ Marcello Coreno,^{7,8} Alberto De Fanis,⁶ Michele Di Fraia,⁸ Benjamin Erk,⁵ Mathieu Gisselbrecht,⁹ Patrik Grychtol,⁶ Per Eng-Johnsson,⁹ Tommaso Mazza,⁶ Jolijn Onvlee,^{1,3, a)} Yevheniy Ovcharenko,⁶ Jovana Petrović,^{1, b)} Nils Rennhack,⁶ Daniel E. Rivas,⁶ Artem Rudenko,¹⁰ Eckart Rühl,¹¹ Lucas Schwob,⁵ Marc Simon,¹² Florian Trinter,^{13,14} Sergey Usenko,⁶ Joss Wiese,¹ Michael Meyer,⁶ Sebastian Trippel,^{1,3, c)} and Jochen Küpper^{1,3,4, d)}

¹⁾Center for Free-Electron Laser Science CFEL, Deutsches Elektronen-Synchrotron DESY, Notkestr. 85, 22607 Hamburg, Germany

²⁾Institute of Atomic and Molecular Physics, Jilin University, Changchun 130012, China

³⁾Center for Ultrafast Imaging, Universität Hamburg, Luruper Chaussee 149, 22761 Hamburg, Germany

⁴⁾Department of Physics, Universität Hamburg, Luruper Chaussee 149, 22761 Hamburg, Germany

⁵⁾Deutsches Elektronen-Synchrotron DESY, Notkestr. 85, 22607 Hamburg, Germany

⁶⁾European XFEL, Holzkoppel 4, 22869 Schenefeld, Germany

⁷⁾ISM-CNR, Istituto Struttura della Materia, LD2 Unit, Basovizza Area Science Park, 34149 Trieste, Italy

⁸⁾Elettra-Sincrotrone Trieste S.C.P.A., 34149 Basovizza, Trieste, Italy

⁹⁾Department of Physics, Lund University, 22100 Lund, Sweden

¹⁰⁾J. R. Macdonald Laboratory, Department of Physics, Kansas State University, Manhattan, Kansas 66506, USA

¹¹⁾Physical Chemistry, Freie Universität Berlin, Arnimallee 22, 14195 Berlin, Germany

¹²⁾Sorbonne Université, CNRS, Laboratoire de Chimie Physique-Matière et Rayonnement, LCPMR, F-75005 Paris, France

¹³⁾Molecular Physics, Fritz-Haber-Institut der Max-Planck-Gesellschaft, Faradayweg 4-6, 14195 Berlin, Germany

¹⁴⁾Institut für Kernphysik, Goethe-Universität Frankfurt, Max-von-Laue-Str. 1, 60438 Frankfurt am Main, Germany

A permanently available molecular-beam injection setup for controlled molecules (COMO) was installed and commissioned at the small quantum systems (SQS) instrument at the European x-ray free-electron laser (EuXFEL). A *b*-type electrostatic deflector allows for pure state-, size-, and isomer-selected samples of polar molecules and clusters. The source provides a rotationally cold ($T \approx 1$ K) and dense ($\rho \approx 10^8$ cm $^{-3}$) molecular beam with pulse durations up to 100 μ s generated by a new version of the Even-Lavie valve. Here, a performance overview of the COMO setup is presented along with characterization experiments performed both, with an optical laser at the Center for Free-Electron-Laser Science and with x-rays at EuXFEL under burst-mode operation. COMO was designed to be attached to different instruments at the EuXFEL, in particular at the small quantum systems (SQS) and single particles, clusters, and biomolecules (SPB) instruments. This advanced controlled-molecules injection setup enables XFEL studies using highly defined samples with soft and hard x-ray FEL radiation for applications ranging from atomic, molecular, and cluster physics to elementary processes in chemistry and biology.

X-ray free-electron lasers (XFELs) deliver x-ray flashes with unprecedentedly high intensities in combination with ultra-short pulse durations down to the attosecond regime.^{1–9} With the development and enormous scientific success of these large-scale light sources such as the free-electron laser in Hamburg (FLASH), the linac coherent light source (LCLS), the free-electron laser radiation for multidisciplinary investigations (FERMI), the SPring-8 Angstrom compact free-electron laser (SACLA), the x-ray free-electron laser at the Paul Scherrer Institute (SwissFEL), the European x-ray free-electron laser (EuXFEL),

and the Shanghai soft x-ray free-electron laser (SXFEL), a huge demand for user experiments arose.^{10–14} In this context, applications with very cold and very pure gas-phase molecular beams are highly desirable, especially for experiments performed in the field of atomic, molecular, and optical (AMO) sciences.^{15–21}

Molecular beam methods were established to obtain fundamental insights into the mechanisms and dynamics of elementary molecular and chemical processes. Starting with the first experiments,^{22,23} molecular beam methods were further developed and refined over the last hundred years and led to tremendous advances in the scientific understanding and manipulation of small molecules in the gas phase. Highlights include the discovery of the intrinsic spin,²⁴ the discovery of nuclear magnetic moments,^{25,26} the investigation of chemical reaction dynamics,²⁷ and the invention of the MASER.²⁸ In particular, in recent years the control of molecules with external fields opened the door to completely new experiments such as scattering experiments at very small relative energies where quantum effects predominate.^{29–34} Using the electrostatic

^{a)}Current address: Radboud University, Institute for Molecules and Materials, Heijendaalseweg 135, 6525 AJ Nijmegen, The Netherlands

^{b)}Current address: Vinča Institute of Nuclear Sciences, National Institute of the Republic of Serbia, University of Belgrade, 12-14 Mike Petrovića Alasa, 11351 Vinča, Belgrade, Serbia

^{c)}sebastian.trippel@cfel.de

^{d)}jochen.kuepper@cfel.de; <https://www.controlled-molecule-imaging.org>

deflector, pure beams of state-, size-, and isomer-selected samples of polar molecules and clusters were realized.^{35–40} Furthermore, due to their rotational temperature on the order of 0.1 K, these pure samples enable very strong laser alignment and mixed field orientation,^{41–45} which can be exploited in the recording of so-called molecular movies, e.g., time-resolved diffractive imaging in the molecular frame to directly determine the molecular structure and dynamics by mathematical transformations from the measured diffraction patterns.^{46–51}

Facilities like FLASH, EuXFEL, or LCLS-II, with repetition rates up to 4.5 MHz, provide ultrashort x-ray pulses with brilliances that are a billion times higher than that of the best conventional x-ray radiation sources.^{3,9,52,53} To match the burst-mode operation of the light pulses at EuXFEL, a cold, pure, and pulsed molecular beam with a duration on the order of 400 μ s and a fundamental repetition rate of 10 Hz is desirable. Therefore, the COMO setup was developed as a permanently available extension of endstations at the SQS and SPB instruments at EuXFEL. COMO is designed based on the concept of a supersonic-molecular-beam source combined with the electrostatic *b*-type deflector.^{48,54}

Here, we present an overview of the design and the capabilities of the permanently available endstation-extension COMO as demonstrated at the SQS instrument of the EuXFEL, where COMO serves as a source for species-selected, cold, dense, and ultra-pure molecular beams.

I. APPARATUS DESCRIPTION

A. Vacuum system

The vacuum setup, shown schematically in the lower right corner of FIG. 1, consists of two stainless steel chambers, highlighted by the blue and purple areas, housing the molecular beam source and the electrostatic *b*-type deflector, respectively. The source chamber is pumped with two turbomolecular pumps (Pfeiffer Vacuum HiPace 2300), resulting in a pumping speed on the order of 4000 L/s for helium. The deflector chamber is pumped with two turbomolecular pumps (Pfeiffer Vacuum HiPace 700), resulting in a pumping speed on the order of 1400 L/s. The typical pressure in the source- and deflector chamber when operating the molecular beam valve at 10 Hz is $\sim 10^{-7}$ and $\sim 10^{-8}$ mbar, respectively. Both chambers can be separated with a manual DN250 CF gate valve (VAT 10848-CE01-0008) to allow for sample changes in the source chamber without breaking the vacuum of the deflector chamber and the endstation. The source chamber is equipped with a quick access door (Pfeiffer Vacuum 420KTU250) on a DN250 CF flange to allow for fast sample replacement in the valve's sample container.⁵⁵ The source and deflector chambers are mounted on rails attached to a stainless steel platform to facilitate easy connection of the entire setup to the endstation. The total mass of the molecular beam setup including the

pumps is ~ 500 kg. The interface between COMO and an endstation requires a DN250 CF port with a cylindrical shaped space with a length of 13.5 cm and a diameter of 20.4 cm inside the endstation for the inverse skimmer pot.

B. Molecular beam setup

A schematic of the COMO molecular beam setup is shown in FIG. 1. A commercially available long-pulse version of an Even-Lavie (EL) valve⁵⁵ is used to deliver the molecular beam by a supersonic expansion of helium with a trace of molecules into the vacuum. This version of the valve produces molecular beam pulse durations up to 100 μ s by utilizing two current pulses in close succession provided by a modified driver unit. The valve is situated on a 3D manipulator (VAB PM12-300-S2EC) with travel ranges of 1.25 cm, 1.25 cm, and 30 cm in *x*, *y*, and *z* directions, respectively. The valve body can be heated up to 250 °C to allow for vapor pressure control of the sample under investigation. Helium is usually used as the carrier gas with a stagnation pressure on the order of tens of bars, up to 100 bar, to generate a cold molecular beam. At EuXFEL, the valve is operated at 10 Hz, matching the x-ray burst rate. A fast beam flux monitor (MBE-Komponenten BFM 40-150) mounted on a DN40 CF linear feedthrough with a linear travel of 15 cm is used to monitor the temporal profile of the molecular beam. The beam flux monitor is controlled by a modified pressure gauge controller (JEVATEC VCU-B0) that allows for measuring the collector current. The collector current is transimpedance amplified with a current amplifier (FEMTO DHPA-100), which in turn is connected to a digitizer to display and record the temporal profile of the molecular beam.

All of the components used to shape the molecular beam are mounted on motorized translation stages and the individual positions can be remotely controlled in planes perpendicular to the molecular beam propagation direction. The first skimmer (Beam Dynamics 50.8, $\varnothing = 3$ mm) is used for differential pumping. The distance between the first skimmer and the valve can be adjusted between 16.5 and 46.5 cm by moving the valve along the molecular beam propagation direction. The first skimmer is mounted on a home-built flange with a built-in 2D translation stage to adjust the skimmer position in the *x* and *y* directions using two stepper motors (Thorlabs, DRV014) outside vacuum and linear feedthroughs. The second skimmer (Beam Dynamics 40.5, $\varnothing = 1.5$ mm) is placed 9.5 cm behind the first skimmer tip for further collimation of the beam. An electrostatic *b*-type deflector,⁵⁴ which disperses the molecules in the beam with respect to their quantum states^{31,56} is located 4.4 cm downstream the tip of the second skimmer. Both electrodes of the electrostatic deflector are connected through two high-voltage feedthroughs (Pfeiffer, 420XST040-30-30-1) allowing for voltages differences up to 60 kV between the electrodes.

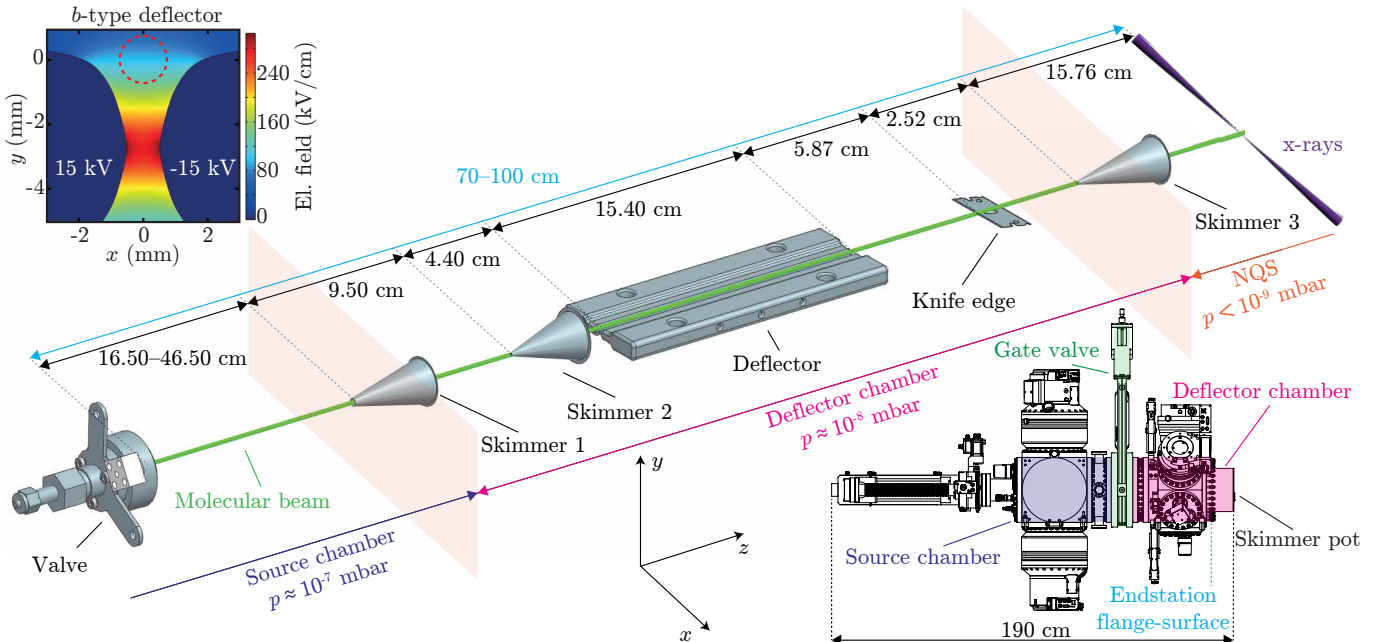


FIG. 1. Schematic of the COMO setup with its main constituents of a pulsed valve and the electrostatic *b*-type deflector. X-rays and possibly further optical laser beams cross the molecular beam in the interaction region of, for example, the NQS endstation at the SQS instrument. Semi-transparent planes indicate differential pumping sections at the first and third skimmer, respectively. The indicated pressures are typical values during operation with long pulses at 10 Hz. The complete COMO vacuum setup is sketched in the lower right corner. The flange surface of an endstation is indicated by the light blue dashed line. The skimmer pot ranges into the endstation. The upper left inset depicts the shape and electric fields of the *b*-type deflector geometry. The numerically calculated electric field strengths are depicted in color coding. The dashed circle indicates the typical size and position of the undeflected molecular beam.

The unit of the second skimmer and the electrostatic deflector are mounted on a 2D translation stage to adjust their positions simultaneously in the *x* and *y* directions using two stepper motors (Thorlabs DRV014) and linear feedthroughs. This translation stage is mounted on the back side of the same flange as the translation stage for skimmer 1. The upper left inset of FIG. 1 depicts the shape and electric fields of the *b*-type deflector geometry. The numerically calculated electric field strengths are depicted in color coding. The dashed circle indicates the typical size and position of the undeflected molecular beam. The dispersed molecular beam is then cut by a vertically adjustable knife edge placed 5.87 cm downstream of the exit of the deflector. This allows for both, improved sample separation and higher column density of the molecular beam.³⁷ The orientation of the knife edge can be controlled by a motorized rotation stage (Smaract SR-1908) to ensure a molecular beam-cut parallel to the x-ray propagation direction. The vertical position of the knife edge can be adjusted by a linear in-vacuum piezo stage (Smaract SLC 1750) with a travel range of 3.1 cm. The typical pressure in the deflector chamber is on the order of 10^{-8} mbar in operation. The molecular beam is further skimmed by a third conical skimmer (Beam Dynamics 50.8, $\varnothing = 1.5$ mm) placed 2.52 cm downstream of the knife edge, providing differential pumping against the interaction chamber. This third skimmer is again

mounted on a 2D translation stage, with the position controlled by two linear in-vacuum piezo stages (Smaract SLC 1750). Behind the third skimmer, the molecular beam enters an endstation compatible with COMO, e.g., the nano-size quantum systems (NQS), or the reaction microscope (REMI) experimental stations at the SQS instrument at EuXFEL.^{9,57} The distance between the tip of the third skimmer and the interaction region with the x-rays is 15.76 cm in case of the NQS setup.

II. CHARACTERIZATION OF THE SETUP

A. Molecular beam temporal profile

To characterize the performance of the COMO setup in-house before its delivery to EuXFEL, it was combined with a time-of-flight mass spectrometer (TOF-MS, Jordan C-677) and tested with a Ti:Sapphire femtosecond laser system (Coherent Astrella) to strong-field-ionize the sample. The laser pulses with a duration of $\text{FWHM}_I \sim 30$ fs and a wavelength centered at 800 nm were focused to $\text{FWHM}_I \approx 50$ μm and directed perpendicular to the molecular beam along the negative *x* direction to ionize molecules in the extraction region of the TOF-MS. The TOF-MS had a distance of 17.6 cm with respect to

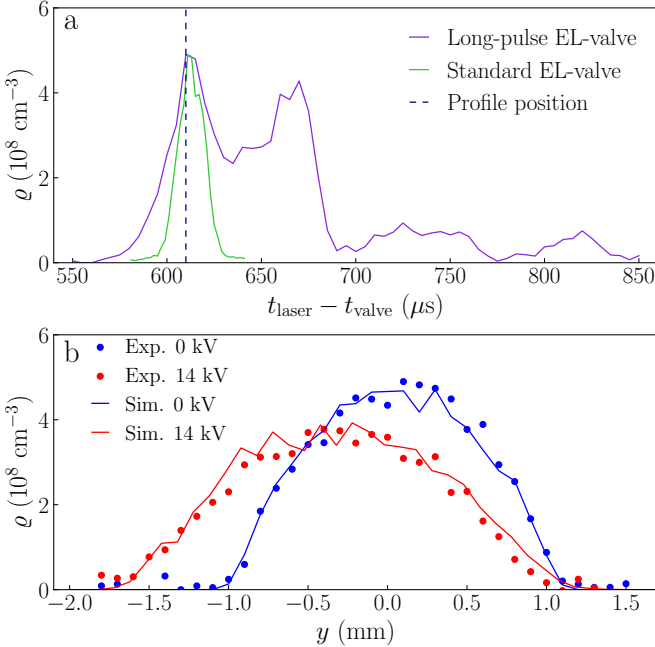


FIG. 2. (a) Temporal molecular-beam-density profiles provided by a long-pulse EL valve (violet) and a normal EL valve (green) obtained from pyrrole⁺. The density of the normal EL valve is not to scale. The dashed line indicates the relative timing where the spatial molecular beam density profiles were measured. (b) Spatial molecular-beam-density profiles for the deflector switched off (blue) and on (red) at a stagnation pressure of 20 bar and a probe time of 610 μs .

the last skimmer tip along the z direction, reflecting the geometry at the EuXFEL SQS instrument. The peak intensity of the laser pulse was $I_0 \sim 6 \times 10^{13} \text{ W/cm}^2$. We used pyrrole as a sample to characterize the temporal and spatial profiles of the molecular beam.⁵⁸ Pyrrole (Sigma-Aldrich Chemie GmbH, 131709) was placed in the sample reservoir of the valve and heated up to 70 °C, which resulted in a pyrrole vapor pressure on the order of 100 mbar.⁵⁹ Helium was used as the carrier gas at a stagnation pressure of 20 bar.

FIG. 2 (a) shows the temporal density profiles of molecular-beam pulses obtained, gating the signal on the parent cation of pyrrole ($m/q = 67 \text{ u/e}$), for both, a long-pulse (violet) and a standard EL valve (green). A pulse duration of $\tau \sim 100 \mu\text{s}$ is observed for the long-pulse valve in contrast to $\tau \sim 25 \mu\text{s}$ in the case of the normal EL valve. In addition, for the long-pulse EL valve, two maxima can be identified during the pulse, resulting from the two current pulses of the driver unit. Furthermore, post pulses were detected at delays between 700–850 μs , which are attributed to the bouncing of the plunger in the EL valve driven by the two current pulses. The post pulses are expected to gradually disappear with increasing stagnation pressure.⁶⁰ The absolute density for the long-pulse EL valve was determined by a laser-pulse-energy scan as described below. The density of the normal EL valve is

not to scale, but from a signal strengths comparison, we assume similar densities as obtained for the long-pulse EL valve.

B. Molecular beam spatial profiles

To characterize the separation of pyrrole from the direct molecular beam, measurements were carried out with and without voltages on the deflector. FIG. 2 (b) shows the measured (dots) and simulated³¹ (lines) profiles for the direct (deflector off, blue) and the 14 kV ($\pm 7 \text{ kV}$) deflected (red) molecular beams. Both profiles were obtained by scanning the molecular beam along the y direction making use of the motorized translation stages to move the beam with respect to the laser propagation axis. The parent ion yields were obtained by integrating over the pyrrole⁺ peak in the TOF-MS. The timing of the laser pulses with respect to the molecular-beam-valve trigger was 610 μs , as indicated by the vertical dashed line in FIG. 2 (a). Comparing both profiles, a clear shift toward negative y values is observed when the deflector is switched on. This is expected, as all quantum states of pyrrole are strong-field seeking at the relevant electric field strengths in the deflector.⁵⁸ The solid lines in FIG. 2 (b) are simulated pyrrole beam profiles obtained from Monte-Carlo trajectory calculations that take into account the geometrical constraints of the mechanical apertures and the rotational temperature T_{rot} of the molecular beam.^{58,61} The experimental data of pyrrole's deflection profiles match well with the simulated results, which assume an initial temperature of $T_{\text{rot}} = 1 \text{ K}$ for the molecular beam entering the deflector. Furthermore, the results are comparable to those obtained in earlier measurements.^{58,62}

C. Molecular beam density determination

The pyrrole molecular beam sample densities were estimated based on a strong-field ionization model.^{62–64} The asymptotic slope of an integral ionization signal with respect to the natural logarithm of peak intensity can be expressed as $S = \varrho \pi R^2 D \alpha$. Here, ϱ represents the sample density, R the I_0/e radius of the transverse laser intensity distribution, D the length of the focal volume in the molecular beam, and α the detection efficiency. The detected number of pyrrole ions per laser pulse as a function of the logarithm of the laser peak intensity $\ln(I_0)$ is shown in FIG. 3. The vertical laser position, molecular beam timing, and stagnation pressure was $y = 0 \text{ mm}$, $t = 600 \mu\text{s}$, and 90 bar, respectively. A typical increase and saturation behavior of the ion yield with increasing laser intensity is observed. The purple curve depicts a fit to the asymptotic slope. From the fit, a saturation onset of $I_0 = (6.8 \pm 1.1_{\text{syst}}) \times 10^{13} \text{ W/cm}^2$ was deduced. A sample density of $\varrho = (8.4 \pm 4.2_{\text{syst}}) \times 10^7 \text{ cm}^{-3}$ was obtained, taking into account the measured laser-beam waist of $\omega_0 = 2\sigma = 52(2) \mu\text{m}$, the measured molecular

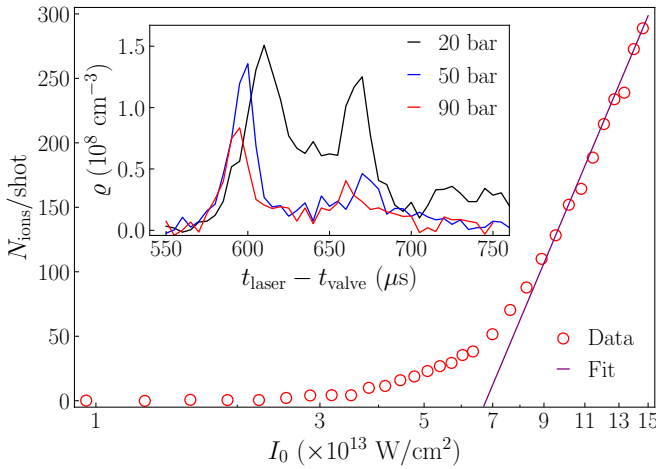


FIG. 3. Number of pyrrole ions per laser pulse (red circles) as a function of the laser peak-intensity logarithm $\ln(I_0)$ for a stagnation pressure of 90 bar. The purple line indicates the asymptotic-slope fit, see text for details. The inset shows temporal molecular-beam-density profiles under different valve stagnation pressures of 20 bar (black), 50 bar (blue), and 90 bar (red).

beam diameter of $D = 2.0(3)$ mm, and an estimated detection efficiency of 50%.⁶⁵ The measured molecular beam density is consistent with typical previously reported values^{48,62,64} obtained with an EL valve. The inset in FIG. 3 shows the temporal profiles of the pyrrole molecular beam for stagnation pressures of 20, 50, and 90 bar, respectively. A decrease in pulse duration is observed with increasing stagnation pressure accompanied by a reduction in peak density. Currently, this limits the long-pulse operation to samples where sufficient cooling is achieved at 20 bar stagnation pressure. Improvements in the valve-driving-electronics parameters are foreseen for samples of controlled and species-selected molecular clusters^{40,58,66} or applications of strong molecular orientation,^{42,67} which require higher stagnation pressures for efficient formation or cooling.

D. Characterization experiments with x-rays

The COMO setup was assembled and further tested with the nano-sized quantum systems (NQS) experimental station at the SQS instrument at EuXFEL. A pure pyrrole-water (PW) heterodimer sample^{58,62} was investigated. The molecular beam was produced using a stagnation pressure of 80 bar of helium with traces of water and pyrrole added. The driver settings were similar to the ones used during the characterization measurements with the optical laser described above. These conditions resulted in a similar spatial molecular beam profile and a purity of pyrrole-water heterodimer as published previously^{58,62} and also shown in FIG. 2 (b). The EuXFEL and the optical laser were operated in burst mode at a base frequency

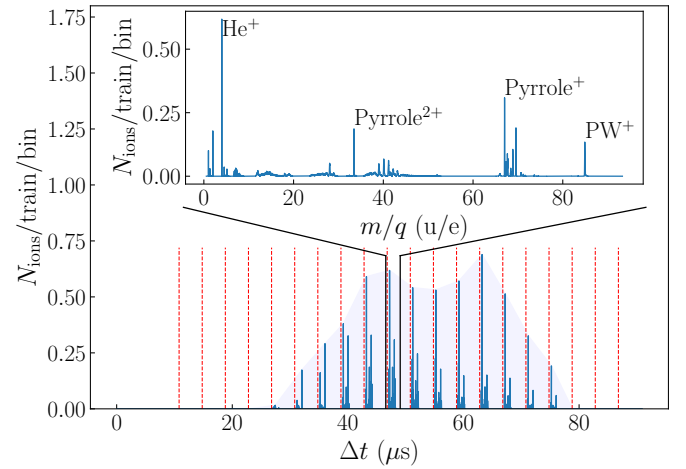


FIG. 4. Ion-yield spectrum induced by the combination of FEL- and 1030 nm optical laser pulse trains at a base frequency of 10 Hz with 20 FEL/1030 nm pulses per train at an intra-train repetition rate of 250 kHz and a photon energy of 600 eV. Δt is the relative timing between the molecular beam arrival time and the train of x-ray pulses. Red vertical dotted lines indicate the arrival of each FEL/1030 nm pulse in the train. The blue shaded area indicates the temporal envelope of the molecular beam density. One bin corresponds to 1.136 ns. The inset is a zoomed-in TOF-MS spectrum corresponding to one of the FEL/1030 nm pulses with the main peaks labeled.

of 10 Hz with 20 FEL pulses, synchronized to the same number of 1030 nm optical laser pulses, per train at an intra-train repetition rate of 250 kHz and a photon energy of 600 eV. FIG. 4 depicts the typical ion-yield spectrum as a function of the relative timing Δt between the molecular beam arrival time and the train of combined x-ray- and 1030 nm optical laser pulses. Vertical red dotted lines indicate the timing of each specific x-ray pulse in the train. The signal envelope as depicted by the blue shaded area indicates the overall temporal profile of the molecular beam in the deflected part. The pulse duration of the molecular beam was on the order of 40 μ s during the commissioning time. The temporal molecular-beam profile is fully covered by the 20 FEL/1030 nm pulses and the specific molecular beam TOF spectra and the background are detected simultaneously in one pulse train. The shorter pulse duration with respect to the duration obtained with the laser shown in FIG. 3 is attributed to the 80 bar stagnation pressure required to produce pyrrole-water clusters at high density.

The inset in FIG. 4 shows a zoomed-in TOF-MS spectrum. The complete, integrated time trace was split into individual traces to obtain a TOF spectrum for each specific x-ray pulse. Afterward, the TOF spectrum corresponding to a specific x-ray pulse was converted to the mass-over-charge ratio in units of u/e . The main ion peaks of the TOF-MS spectrum are labeled and attributed to the pyrrole-water parent ion (PW^+), pyrrole-water fragment ions, and remaining seed gas contributions (He^+). A detailed analysis of the TOF-MS spectrum is beyond the

scope of this paper and will be discussed in a future publication. However, all ion signals induced by the x-rays can be clearly resolved in the TOF-MS spectrum, demonstrating that the COMO setup is fully compatible with the chosen burst mode operation at the EuXFEL. This will significantly increase the data-acquisition duty cycle, and thus the utilization of x-ray pulses, compared to experiments using standard short-pulse valves up to a factor of ~ 4 . It should be mentioned here that there are no relevant restrictions on the number of pulses with which the valve is operated, up to several hundred pulses per second. By modifying the electric driver longer molecular pulses will be possible to cover the 400 μs duration of EuXFEL pulse trains. Furthermore, our results demonstrate that the obtained molecular sample densities are clearly sufficient to conduct experiments with x-rays at free-electron lasers using COMO. In addition, exploiting the electrostatic deflector, the x-ray induced helium-ion signal, from the molecular beam seed gas, is highly suppressed. However, to implement 100 μs or longer molecular beam pulses under conditions to produce significant densities of molecular clusters, further optimization of the valve performance is required.

III. CONCLUSION

In summary, the permanently available molecular-beam injector setup COMO was developed, set up, and commissioned using TOF-MS experiments both in-house at CFEL with optical-laser-ionization and at EuXFEL with x-ray-ionization detection. The performance of the long-pulse-valve molecular-beam source was characterized and proven to be compatible with the burst mode operation of the EuXFEL. Our results show that the COMO setup can generate cold ($T \sim 1 \text{ K}$) and dense ($\rho \sim 10^8 \text{ cm}^{-3}$) molecular-beam pulses with pulse durations on the order of 100 μs . The high molecular beam density allows experiments with data recorded in single-shot mode. In general, the COMO molecular beam source can be combined with various electron- and ion-spectrometers, along with large-area x-ray detectors. With the included electrostatic deflector, pure state-, size-, and isomer-selected samples of polar molecules and clusters can be provided to the interaction region.

Hence, COMO proves to be an excellent source for various experiments at the EuXFEL, such as the recording of molecular movies using ion, electron, and x-ray imaging. This enables a diverse range of science from atomic, molecular, and cluster physics to materials and energy science, as well as chemistry and biology.

IV. ACKNOWLEDGMENTS

We gratefully acknowledge Uzi Even, Nachum A. Lavia, and Ronny Barnea for designing and making commercially

available the long-pulse Even-Lavia valve and for sharing early test results from their laboratory.

We acknowledge financial support by Deutsches Elektronen-Synchrotron DESY, a member of the Helmholtz Association (HGF), the Clusters of Excellence “Center for Ultrafast Imaging” (CUI, EXC 1074, ID 194651731) and “Advanced Imaging of Matter” (AIM, EXC 2056, ID 390715994) of the Deutsche Forschungsgemeinschaft (DFG), by the European Research Council under the European Union’s Seventh Framework Program (FP7/2007-2013) through the Consolidator Grant COMOTION (614507), the European Union’s Horizon 2020 research and innovation programme under the Marie Skłodowska-Curie Grant Agreement “Molecular Electron Dynamics investigated by Intense Fields and Attosecond Pulses” (MEDEA, 641789), the Helmholtz Foundation through funds from the Helmholtz-Lund International Graduate School (HELIOS, Helmholtz project number HIRS-0018), and from the German Federal Ministry of Education and Research (BMBF) and the Swedish Research Council (VR 2021-05992) through the Röntgen-Ångström cluster (project “Ultrafast dynamics in intermolecular energy transfer: elementary processes in aerosols and liquid chemistry” UDIET, 05K22GUA). We also acknowledge the scientific exchange of the Center for Molecular Water Science (CMWS). For the experiments at EuXFEL we acknowledge EuXFEL in Schenefeld, Germany, for the provision of XFEL beam time at the SQS instrument and thank the staff for their assistance.

L.H. acknowledges the support by the National Natural Science Foundation of China (11704147 and 92261201) and a fellowships within the framework of the Helmholtz-OCPC postdoctoral exchange program. F.T. acknowledges funding by the Deutsche Forschungsgemeinschaft (DFG, project 509471550, Emmy-Noether programme) and by the MaxWater initiative of the Max-Planck-Gesellschaft. S.B. and L.S. acknowledge funding by the Helmholtz Initiative and Networking Fund.

V. DATA AVAILABILITY

The data recorded for the experiment at the EuXFEL are available at <https://doi.org/10.22003/XFEL.EU-DATA-002388-00>. The data recorded in the laser lab at DESY are available from the corresponding author upon reasonable request.

VI. CODE AVAILABILITY

The code for the data analysis is available from the corresponding author upon reasonable request.

¹B. W. J. McNeil and N. R. Thompson, “X-ray free-electron lasers,” Nat. Photon. **4**, 814–821 (2010).

²P. Emma, R. Akre, J. Arthur, R. Bionta, C. Bostedt, J. Bozek, A. Brachmann, P. Bucksbaum, R. Coffee, F. J. Decker, Y. Ding,

- D. Dowell, S. Edstrom, A. Fisher, J. Frisch, S. Gilevich, J. Hastings, G. Hays, P. Hering, Z. Huang, R. Iverson, H. Loos, M. Messerschmidt, A. Miahnahri, S. Moeller, H. D. Nuhn, G. Pile, D. Ratner, J. Rzepiela, D. Schultz, T. Smith, P. Stefan, H. Tompkins, J. Turner, J. Welch, W. White, J. Wu, G. Yocky, and J. Galayda, "First lasing and operation of an ångstrom-wavelength free-electron laser," *Nat. Photon.* **4**, 641–647 (2010).
- ³M. Altarelli, "The European X-ray free-electron laser facility in Hamburg," *Nucl. Instrum. Methods Phys. Res. Sect. B* **269**, 2845–2849 (2011).
- ⁴T. Ishikawa, H. Aoyagi, T. Asaka, Y. Asano, N. Azumi, T. Bizen, H. Ego, K. Fukami, T. Fukui, Y. Furukawa, S. Goto, H. Hanaki, T. Hara, T. Hasegawa, T. Hatsui, A. Higashiya, T. Hiroto, N. Hosoda, M. Ishii, T. Inagaki, Y. Inubushi, T. Itoga, Y. Joti, M. Kago, T. Kameshima, H. Kimura, Y. Kirihara, A. Kiyomichi, T. Kobayashi, C. Kondo, T. Kudo, H. Maesaka, X. M. Marechal, T. Masuda, S. Matsubara, T. Matsumoto, T. Matsushita, S. Matsui, M. Nagasono, N. Nariyama, H. Ohashi, T. Ohata, T. Ohshima, S. Ono, Y. Otake, C. Saji, T. Sakurai, T. Sato, K. Sawada, T. Seike, K. Shirasawa, T. Sugimoto, S. Suzuki, S. Takahashi, H. Takebe, K. Takeshita, K. Tamásakú, H. Tanaka, R. Tanaka, T. Tanaka, T. Togashi, K. Togawa, A. Tokuhisa, H. Tomizawa, K. Tono, S. Wu, M. Yabashi, M. Yamaga, A. Yamashita, K. Yanagida, C. Zhang, T. Shintake, H. Kitamura, and N. Kumagai, "A compact X-ray free-electron laser emitting in the sub-ångstrom region," *Nat. Photon.* **6**, 540–544 (2012).
- ⁵C. J. Milne, T. Schietinger, M. Aiba, A. Alarcon, J. Alex, A. Anghel, V. Arsov, C. Beard, P. Beaud, S. Bettini, M. Bopp, H. Brands, M. Brönnimann, I. Brunnenkant, M. Calvi, A. Citterio, P. Craievich, M. Csاتari Divall, M. Dällenbach, M. D'Amico, A. Dax, Y. Deng, A. Dietrich, R. Dinapoli, E. Divall, S. Dordevic, S. Ebner, C. Erny, H. Fitze, U. Flechsig, R. Follath, F. Frei, F. Gärtner, R. Ganter, T. Garvey, Z. Geng, I. Gorogisan, C. Gough, A. Hauff, C. P. Hauri, N. Hiller, T. Humar, S. Hunziker, G. Ingold, R. Ischebeck, M. Janousch, P. Juranić, M. Jurcevic, M. Kaiser, B. Kalantari, R. Kalt, B. Keil, C. Kittel, G. Knopp, W. Koprek, H. T. Lemke, T. Lippuner, D. Llorente Sancho, F. Löhl, C. Lopez-Cuenca, F. Märki, F. Marcellini, G. Marinkovic, I. Martiel, R. Menzel, A. Mozzanica, K. Nass, G. L. Orlandi, C. Ozkan Loch, E. Panepucci, M. Paraliev, B. Patterson, B. Pedrini, M. Pedrozzi, P. Pollet, C. Prader-vand, E. Prat, P. Radi, J.-Y. Raguin, S. Redford, J. Rehanek, J. Réhault, S. Reiche, M. Ringele, J. Rittmann, L. Rivkin, A. Romann, M. Ruat, C. Ruder, L. Sala, L. Schebacher, T. Schilcher, V. Schlott, T. Schmidt, B. Schmitt, X. Shi, M. Stadler, L. Stingelin, W. Sturzenegger, J. Szlachetko, D. Thattil, D. M. Treyer, A. Trisorio, W. Tron, S. Vetter, C. Vicario, D. Voulot, M. Wang, T. Zamofing, C. Zellweger, R. Zennaro, E. Zimoch, R. Abela, L. Patthey, and H.-H. Braun, "SwissFEL: The Swiss X-ray Free Electron Laser," *Appl. Sci.* **7**, 720 (2017).
- ⁶H.-S. Kang, C.-K. Min, H. Heo, C. Kim, H. Yang, G. Kim, I. Nam, S. Y. Baek, H.-J. Choi, G. Mun, B. R. Park, Y. J. Suh, D. C. Shin, J. Hu, J. Hong, S. Jung, S.-H. Kim, K. Kim, D. Na, S. S. Park, Y. J. Park, J.-H. Han, Y. G. Jung, S. H. Jeong, H. G. Lee, S. Lee, S. Lee, W.-W. Lee, B. Oh, H. S. Suh, Y. W. Parc, S.-J. Park, M. H. Kim, N.-S. Jung, Y.-C. Kim, M.-S. Lee, B.-H. Lee, C.-W. Sung, I.-S. Mok, J.-M. Yang, C.-S. Lee, H. Shin, J. H. Kim, Y. Kim, J. H. Lee, S.-Y. Park, J. Kim, J. Park, I. Eom, S. Rah, S. Kim, K. H. Nam, J. Park, J. Park, S. Kim, S. Kwon, S. H. Park, K. S. Kim, H. Hyun, S. N. Kim, S. Kim, S.-m. Hwang, M. J. Kim, C.-y. Lim, C.-J. Yu, B.-S. Kim, T.-H. Kang, K.-W. Kim, S.-H. Kim, H.-S. Lee, H.-S. Lee, K.-H. Park, T.-Y. Koo, D.-E. Kim, and I. S. Ko, "Hard X-ray free-electron laser with femtosecond-scale timing jitter," *Nat. Photon.* **11**, 708–713 (2017).
- ⁷E. Allaria, D. Castronovo, P. Cinquegrana, P. Craievich, M. Dal Forno, M. B. Danailov, G. D'Auria, A. Demidovich, G. De Ninno, S. Di Mitri, B. Diviacco, W. M. Fawley, M. Ferianis, E. Ferrari, L. Froehlich, G. Gaio, D. Gauthier, L. Giannessi, R. Ivanov, B. Mahieu, N. Mahne, I. Nikolov, F. Parmigiani, G. Penco, L. Raimondi, C. Scafuri, C. Serpico, P. Sigalotti, S. Spampinati, C. Spezzani, M. Svandrlík, C. Svetina, M. Trovo, M. Veronese, D. Zangrandi, and M. Zangrandi, "Two-stage seeded soft-X-ray free-electron laser," *Nat. Photon.* **7**, 913–918 (2013).
- ⁸N. Hartmann, G. Hartmann, R. Heider, M. S. Wagner, M. Ilchen, J. Buck, A. O. Lindahl, C. Benko, J. Grünert, J. Krzywinski, J. Liu, A. A. Lutman, A. Marinelli, T. Maxwell, A. A. Miahnahri, S. P. Moeller, M. Planas, J. Robinson, A. K. Kazansky, N. M. Kabachnik, J. Viehaus, T. Feurer, R. Kienberger, R. N. Coffee, and W. Helml, "Attosecond time-energy structure of X-ray free-electron laser pulses," *Nat. Photon.* **12**, 215–220 (2018).
- ⁹W. Decking, S. Abeghyan, P. Abramian, A. Abramsky, A. Aguirre, C. Albrecht, P. Alou, M. Altarelli, P. Altmann, K. Amyan, V. Anashin, E. Apostolov, K. Appel, D. Auguste, V. Ayvazyan, S. Baark, F. Babies, N. Baboi, P. Bak, V. Balandin, R. Baldinger, B. Baranasic, S. Barbanotti, O. Belikov, V. Belokurov, L. Belova, V. Belyakov, S. Berry, M. Bertucci, B. Beutner, A. Block, M. Blöcher, T. Böckmann, C. Bohm, M. Böhner, V. Bondar, E. Bondarchuk, M. Bonezzi, P. Borowiec, C. Bösch, U. Bösenberg, A. Bosotti, R. Böspflug, M. Bousonville, E. Boyd, Y. Bozhko, A. Brand, J. Branlard, S. Brieche, F. Brinker, S. Brinker, R. Brinkmann, S. Brockhauser, O. Brovko, H. Brück, A. Brüdgam, L. Butkowski, T. Büttner, J. Calero, E. Castro-Carballo, G. Cat-talanotto, J. Charrier, J. Chen, A. Cherepenko, V. Cheskidov, M. Chiodini, A. Chong, S. Choroba, M. Chorowski, D. Churanov, W. Cichalewski, M. Clausen, W. Clement, C. Cloué, J. A. Cobos, N. Coppola, S. Cunis, K. Czuba, M. Czwalińska, B. D'Almagne, J. Dammann, H. Danared, A. d. Z. Wagner, A. Delfs, T. Delfs, F. Dietrich, T. Dietrich, M. Dohlus, M. Domnach, A. Donat, X. Dong, N. Doynikov, M. Dressel, M. Duda, P. Duda, H. Eckoldt, W. Ehsan, J. Eidam, F. Eints, C. Engling, U. Englisch, A. Er-makov, K. Escherich, J. Eschke, E. Saldin, M. Faesing, A. Fallou, M. Felber, M. Fenner, B. Fernandes, J. M. Fernández, S. Feuker, K. Filippakopoulos, K. Floettmann, V. Fogel, M. Fontaine, A. Francés, I. F. Martin, W. Freund, T. Freyer-muth, M. Fried-land, L. Fröhlich, M. Fusetti, J. Fydrych, A. Gallas, O. García, L. Garcia-Tabares, G. Geloni, N. Gerasimova, C. Gerth, P. Geßler, V. Gharibyan, M. Gloor, J. Główkowski, A. Goessel, Z. Gołębiewski, N. Golubeva, W. Grabowski, W. Graeff, A. Grebentsov, M. Grecki, T. Grevsmuehl, M. Gross, U. Grosse-Wortmann, J. Grünert, S. Grunewald, P. Grzegory, G. Feng, H. Guler, G. Gusev, J. L. Gutierrez, L. Hagge, M. Hamberg, R. Hanneken, E. Harms, I. Hartl, A. Hauberg, S. Hauf, J. Hauschildt, J. Hauser, J. Havlicek, A. Hedqvist, N. Heidbrook, F. Hellberg, D. Henning, O. Hensler, T. Hermann, A. Hidvégi, M. Hierholzer, H. Hintz, F. Hoffmann, M. Hoffmann, M. Hoffmann, Y. Holler, M. Hüning, A. Ignatenko, M. Ilchen, A. Iluk, J. Iversen, J. Iversen, M. Izquierdo, L. Jachmann, N. Jardon, U. Jastrow, K. Jen-sch, J. Jensen, M. Ježábel, M. Jidda, H. Jin, N. Johansson, R. Jonas, W. Kaabi, D. Kaefer, R. Kammering, H. Kapitza, S. Karabekyan, S. Karstensen, K. Kasprzak, V. Katalev, D. Keese, B. Keil, M. Kholopov, M. Killenberger, B. Kitaev, Y. Klimchenko, R. Klos, L. Knebel, A. Koch, M. Koepke, S. Köhler, W. Köhler, N. Kohlstrunk, Z. Konopkova, A. Konstantinov, W. Kook, W. Koprek, M. Körfer, O. Korth, A. Kosarev, K. Kosiński, D. Kostin, Y. Kot, A. Kotarba, T. Kozak, V. Kozak, R. Kramert, M. Krasilnikov, A. Krasnov, B. Krause, L. Kravchuk, O. Krebs, R. Kretschmer, J. Kreutzkamp, O. Kröplin, K. Krzysik, G. Kube, H. Kuehn, N. Kujala, V. Kulikov, V. Kuzminych, D. L. Civita, M. Lacroix, T. Lamb, A. Lancetov, M. Larsson, D. L. Pin-vidic, S. Lederer, T. Lensch, D. Lenz, A. Leuschner, F. Lev-enhagen, Y. Li, J. Liebing, L. Lilje, T. Limberg, D. Lipka, B. List, J. Liu, S. Liu, B. Lorbeer, J. Lorkiewicz, H. H. Lu, F. Ludwig, K. Machau, W. Maciocha, C. Madec, C. Maguer, C. Mafiano, I. Maksimova, K. Malcher, T. Maltezopoulos, E. Mamoshkina, B. Manschuetus, F. Marcellini, G. Marinkovic, T. Martinez, H. Martirosyan, W. Maschmann, M. Maslov, A. Math-eisen, U. Mavric, J. Meißner, K. Meissner, M. Messerschmidt, N. Meyners, G. Michalski, P. Michelato, N. Mildner, M. Moe, F. Moglia, C. Mohr, S. Mohr, W. Möller, M. Mommerz, L. Monaco,

- C. Montiel, M. Moretti, I. Morozov, P. Morozov, D. Mross, J. Mueller, C. Müller, J. Müller, K. Müller, J. Munilla, A. Münnich, V. Muratov, O. Napoly, B. Näser, N. Nefedov, R. Neumann, R. Neumann, N. Ngada, D. Noelle, F. Obier, I. Okunev, J. A. Oliver, M. Omet, A. Oppelt, A. Ottmar, M. Oublaid, C. Pagani, R. Paparella, V. Paramonov, C. Peitzmann, J. Penning, A. Perus, F. Peters, B. Petersen, A. Petrov, I. Petrov, S. Pfeiffer, J. Pfleiderer, S. Philipp, Y. Piennaud, P. Pierini, S. Pivovarov, M. Planas, E. Pławski, M. Pohl, J. Polinski, V. Popov, S. Prat, J. Prenting, G. Priebe, H. Pryschelski, K. Przygoda, E. Pyata, B. Racky, A. Rathjen, W. Ratuschni, S. Regnaud-Campderros, K. Rehlich, D. Reschke, C. Robson, J. Roever, M. Roggli, J. Rothenburg, E. Rusiński, R. Rybaniec, H. Sahling, M. Salmani, L. Samoylova, D. Sanzone, F. Saretzki, O. Sawlanski, J. Schaffran, H. Schlarb, M. Schlösser, V. Schlott, C. Schmidt, F. Schmidt-Foehre, M. Schmitz, M. Schmökel, T. Schnautz, E. Schneidmiller, M. Scholz, B. Schöneburg, J. Schultz, C. Schulz, A. Schwarz, J. Sekutowicz, D. Sellmann, E. Semenov, S. Serkez, D. Sertore, N. Shehzad, P. Shemarykin, L. Shi, M. Sienkiewicz, D. Sikora, M. Sikorski, A. Silenzi, C. Simon, W. Singer, X. Singer, H. Sinn, K. Sinram, N. Skvorodnev, P. Smirnow, T. Sommer, A. Sorokin, M. Stadler, M. Steckel, B. Steffen, N. Steinhau-Kühl, F. Stephan, M. Stodulski, M. Stolper, A. Sulimov, R. Susen, J. Świerblewski, C. Sydlo, E. Syresin, V. Sytchev, J. Szuba, N. Tesch, J. Thie, A. Thiebault, K. Tiedtke, D. Tischhauser, J. Tolkihn, S. Tomin, F. Tonisch, F. Toral, I. Torbin, A. Trapp, D. Treyer, G. Trowitzsch, T. Trublet, T. Tschentscher, F. Ullrich, M. Vannoni, P. Varela, G. Varghese, G. Vashchenko, M. Vasic, C. Vazquez-Velez, A. Verguet, S. Vilcins-Czvitkovits, R. Villanueva, B. Visentin, M. Viti, E. Vogel, E. Volobuev, R. Wagner, N. Walker, T. Wamsat, H. Weddig, G. Weichert, H. Weise, R. Wenndorf, M. Werner, R. Wichmann, C. Wiebers, M. Wiencek, T. Wilksen, I. Will, L. Winkelmann, M. Winkowski, K. Wittenburg, A. Witzig, P. Wlk, T. Wohlenberg, M. Wojciechowski, F. Wolff-Fabris, G. Wrochna, K. Wrona, M. Yakopov, B. Yang, F. Yang, M. Yurkov, I. Zagorodnov, P. Zalden, A. Zavadtsev, D. Zavadtsev, A. Zhirnov, A. Zhukov, V. Zieman, A. Zolotov, N. Zolotukhina, F. Zummack, and D. Zybin, "A MHz-repetition-rate hard X-ray free-electron laser driven by a superconducting linear accelerator," *Nat. Photon.* **14**, 391–397 (2020).
- ¹⁰L. Strüder, S. Epp, D. Rolles, R. Hartmann, P. Holl, G. Lutz, H. Soltau, R. Eckart, C. Reich, K. Heinzinger, C. Thamm, A. Rudenko, F. Krasniqi, K. Kühnel, C. Bauer, C.-D. Schroeter, R. Moshammer, S. Techert, D. Miessner, M. Porro, O. Haelker, N. Meidinger, N. Kimmel, R. Andritschke, F. Schopper, G. Weidenspointner, A. Ziegler, D. Pietschner, S. Herrmann, U. Pietsch, A. Walenta, W. Leitenberger, C. Bostedt, T. Moeller, D. Rupp, M. Adolph, H. Graafsma, H. Hirsemann, K. Gaertner, R. Richter, L. Foucar, R. L. Shoeman, I. Schlichting, and J. Ullrich, "Large-format, high-speed, X-ray pnCCDs combined with electron and ion imaging spectrometers in a multipurpose chamber for experiments at 4th generation light sources," *Nucl. Instrum. Methods Phys. Res. A* **614**, 483–496 (2010).
- ¹¹Z. Zhao, D. Wang, Q. Gu, L. Yin, M. Gu, Y. Leng, and B. Liu, "Status of the SXFEL Facility," *Appl. Sci.* **7**, 607 (2017).
- ¹²L. Young, K. Ueda, M. Gühr, P. H. Bucksbaum, M. Simon, S. Mukamel, N. Rohringer, K. C. Prince, C. Masciovecchio, M. Meyer, A. Rudenko, D. Rolles, C. Bostedt, M. Fuchs, D. A. Reis, R. Santra, H. Kapteyn, M. Murnane, H. Ibrahim, F. Légaré, M. J. J. Vrakking, M. Isinger, D. Kroon, M. Gisselbrecht, A. L'Huillier, H. J. Wörner, and S. R. Leone, "Roadmap of ultrafast x-ray atomic and molecular physics," *J. Phys. B* **51**, 032003 (2018).
- ¹³B. Erk, J. P. Müller, C. Bomme, R. Boll, G. Brenner, H. N. Chapman, J. Correa, S. Düsterer, S. Dzirarhytski, S. Eisebitt, H. Graafsma, S. Grunewald, L. Gumprecht, R. Hartmann, G. Hauser, B. Keitel, C. von Korff Schmising, M. Kuhlmann, B. Manschweitus, L. Mercadier, E. Müller, C. Passow, E. Plönjes, D. Ramm, D. Rompotis, A. Rudenko, D. Rupp, M. Sauppe, F. Siewert, D. Schlosser, L. Strüder, A. Swiderski, S. Techert, K. Tiedtke, T. Tilp, R. Treusch, I. Schlichting, J. Ullrich, R. Moshammer, T. Möller, and D. Rolles, "CAMP@FLASH: an end-station for imaging, electron- and ion-spectroscopy, and pump-probe experiments at the FLASH free-electron laser," *J. Synchrotron Rad.* **25**, 1529–1540 (2018).
- ¹⁴M. Kuster, K. Ahmed, K.-E. Ballak, C. Danilevski, M. Ekmedžić, B. Fernandes, P. Gessler, R. Hartmann, S. Hauf, P. Holl, M. Meyer, J. Montaño, A. Münnich, Y. Ovcharenko, N. Renhack, T. Rüter, D. Rupp, D. Schlosser, K. Setodehnia, R. Schmitt, L. Strüder, R. M. P. Tanyag, A. Ulmer, and H. Yousef, "The 1-Megapixel pnCCD detector for the Small Quantum Systems Instrument at the European XFEL: system and operation aspects," *J. Synchrotron Rad.* **28**, 576–587 (2021).
- ¹⁵L. Young, E. P. Kanter, B. Kraessig, Y. Li, A. M. March, S. T. Pratt, R. Santra, S. H. Southworth, N. Rohringer, L. F. DiMauro, G. Doumy, C. A. Roedig, N. Berrah, L. Fang, M. Hoener, P. H. Bucksbaum, J. P. Cryan, S. Ghimire, J. M. Glownia, D. A. Reis, J. D. Bozek, C. Bostedt, and M. Messerschmidt, "Femtosecond electronic response of atoms to ultra-intense x-rays," *Nature* **466**, 56 (2010).
- ¹⁶B. Rudek, S.-K. Son, L. Foucar, S.-W. Epp, B. Erk, R. Hartmann, M. Adolph, R. Andritschke, A. Aquila, N. Berrah, C. Bostedt, N. Bozek, Johnand Coppola, F. Filsinger, H. Gorke, T. Gorkhov, H. Graafsma, L. Gumprecht, A. Hartmann, G. Hauser, S. Herrmann, H. Hirsemann, P. Holl, A. Hömke, L. Journel, C. Kaiser, N. Kimmel, F. Krasniqi, K.-U. Kühnel, M. Matysek, M. Messerschmidt, D. Miesner, T. Möller, R. Moshammer, K. Nagaya, B. Nilsson, G. Potdevin, D. Pietschner, C. Reich, D. Rupp, G. Schaller, I. Schlichting, C. Schmidt, F. Schopper, S. Schorb, C.-D. Schröter, J. Schulz, M. Simon, H. Soltau, L. Strüder, K. Ueda, G. Weidenspointner, R. Santra, J. Ullrich, A. Rudenko, and D. Rolles, "Ultra-efficient ionization of heavy atoms by intense x-ray free-electron laser pulses," *Nat. Photon.* **6**, 858–865 (2012).
- ¹⁷J. Feldhaus, M. Krikunova, M. Meyer, T. Möller, R. Moshammer, A. Rudenko, T. Tschentscher, and J. Ullrich, "AMO science at the FLASH and European XFEL free-electron laser facilities," *J. Phys. B* **46**, 164002 (2013).
- ¹⁸U. Eichmann, H. Rottke, S. Meise, J.-E. Rubensson, J. Söderström, M. Agäker, C. Säthe, M. Meyer, T. M. Baumann, R. Boll, A. D. Fanis, P. Grychtol, M. Ilchen, T. Mazza, J. Montano, V. Music, Y. Ovcharenko, D. E. Rivas, S. Serkez, R. Wagner, and S. Eisebitt, "Photon-recoil imaging: Expanding the view of nonlinear x-ray physics," *Science* **369**, 1630–1633 (2020).
- ¹⁹X. Li, L. Inhester, S. J. Robatjazi, B. Erk, R. Boll, K. Hanasaki, K. Toyota, Y. Hao, C. Bomme, B. Rudek, L. Foucar, S. H. Southworth, C. S. Lehmann, B. Kraessig, T. Marchenko, M. Simon, K. Ueda, K. R. Ferguson, M. Bucher, T. Gorkhov, S. Caron, R. Alonso-Mori, J. E. Koglin, J. Correa, G. J. Williams, S. Boutet, L. Young, C. Bostedt, S.-K. Son, R. Santra, D. Rolles, and A. Rudenko, "Pulse Energy and Pulse Duration Effects in the Ionization and Fragmentation of Iodomethane by Ultraintense Hard X Rays," *Phys. Rev. Lett.* **127**, 093202 (2021).
- ²⁰K. Fehre, N. M. Novikovskiy, S. Grundmann, G. Kastirke, S. Eckart, F. Trinter, J. Rist, A. Hartung, D. Trabert, C. Janke, G. Nalin, M. Pitzer, S. Zeller, F. Wiegandt, M. Weller, M. Kircher, M. Hofmann, L. P. H. Schmidt, A. Knie, A. Hans, L. B. Tlaief, A. Ehresmann, R. Berger, H. Fukuzawa, K. Ueda, H. Schmidt-Böcking, J. B. Williams, T. Jahnke, R. Dörner, M. S. Schöffler, and P. V. Demekhin, "Fourfold Differential Photoelectron Circular Dichroism," *Phys. Rev. Lett.* **127**, 103201 (2021).
- ²¹J. W. L. Lee, D. S. Tikhonov, P. Chopra, S. Maclot, A. L. Steber, S. Gruet, F. Allum, R. Boll, X. Cheng, S. Düsterer, B. Erk, D. Garg, L. He, D. Heathcote, M. Johnny, M. M. Kazemi, H. Köckert, J. Lahl, A. K. Lemmens, D. Loru, R. Mason, E. Müller, T. Mullins, P. Olshin, C. Passow, J. Peschel, D. Ramm, D. Rompotis, N. Schirmel, S. Trippel, J. Wiese, F. Ziae, S. Bari, M. Burt, J. Küpper, A. M. Rijs, D. Rolles, S. Techert, P. Eng-Johnsson, M. Brouard, C. Vallance, B. Manschwetus, and M. Schnell, "Time-resolved relaxation and fragmentation of polycyclic aromatic hydrocarbons investigated in the ultrafast XUV-IR regime," *Nat.*

- Commun. **12**, 6107 (2021).

²²L. Dunoyer, "Sur la théorie cinétique des gaz et la réalisation d'un rayonnement matériel d'origine thermique," Cr. hebd. séances Acad. sci. **152**, 592–595 (1911).

²³O. Stern, "Zur Methode der Molekularstrahlen I," Z. Phys. **39**, 751–763 (1926).

²⁴O. Stern, "The experimental proof of spatial quantisation in the electrical field," Physikalische Zeitschrift **23**, 476–481 (1922).

²⁵R. Frisch and O. Stern, "Über die magnetische Ablenkung von Wasserstoffmolekülen und das magnetische Moment des Protons. I," Z. Phys. **85**, 4–16 (1933).

²⁶I. I. Rabi, S. Millman, P. Kusch, and J. R. Zacharias, "The molecular beam resonance method for measuring nuclear magnetic moments - the magnetic moments of ${}^3\text{Li}^6$, ${}^3\text{Li}^7$ and ${}^9\text{F}^{19}$," Phys. Rev. **55**, 526–535 (1939).

²⁷D. R. Herschbach, "Reactive collisions in crossed molecular beams," Discuss. Faraday Soc. **33**, 149–161 (1962).

²⁸J. P. Gordon, H. J. Zeiger, and C. H. Townes, "The maser—new type of microwave amplifier, frequency standard, and spectrometer," Phys. Rev. **99**, 1264–1274 (1955).

²⁹S. Y. T. van de Meerakker, H. L. Bethlehem, and G. Meijer, "Taming molecular beams," Nat. Phys. **4**, 595 (2008).

³⁰S. Y. T. van de Meerakker, H. L. Bethlehem, N. Vanhaecke, and G. Meijer, "Manipulation and control of molecular beams," Chem. Rev. **112**, 4828–4878 (2012).

³¹Y.-P. Chang, D. A. Horke, S. Trippel, and J. Küpper, "Spatially-controlled complex molecules and their applications," Int. Rev. Phys. Chem. **34**, 557–590 (2015), arXiv:1505.05632 [physics].

³²A. von Zastrow, J. Onvlee, S. N. Vogels, G. C. Groenenboom, A. van der Avoird, and S. Y. T. van de Meerakker, "State-resolved diffraction oscillations imaged for inelastic collisions of NO radicals with He, Ne and Ar," Nat. Chem. **6**, 216 – 221 (2014).

³³A. B. Henson, S. Gersten, Y. Shagam, J. Narevicius, and E. Narevicius, "Observation of resonances in penning ionization reactions at sub-kelvin temperatures in merged beams," Science **338**, 234–238 (2012).

³⁴J. Jankunas, B. Bertsche, and A. Osterwalder, "Study of the $\text{Ne}({}^3\text{P}_2) + \text{CH}_3\text{F}$ Electron-Transfer Reaction below 1 K," J. Phys. Chem. A **118**, 3875–3879 (2014).

³⁵F. Filsinger, U. Erlekam, G. von Helden, J. Küpper, and G. Meijer, "Selector for structural isomers of neutral molecules," Phys. Rev. Lett. **100**, 133003 (2008), arXiv:0802.2795 [physics].

³⁶F. Filsinger, J. Küpper, G. Meijer, J. L. Hansen, J. Maurer, J. H. Nielsen, L. Holmegaard, and H. Stapelfeldt, "Pure samples of individual conformers: The separation of stereo-isomers of complex molecules using electric fields," Angew. Chem. Int. Ed. **48**, 6900–6902 (2009).

³⁷S. Trippel, M. Johny, T. Kierspel, J. Onvlee, H. Bieker, H. Ye, T. Mullins, L. Gumprecht, K. Dlugolecki, and J. Küpper, "Knife edge skimming for improved separation of molecular species by the deflector," Rev. Sci. Instrum. **89**, 096110 (2018), arXiv:1802.04053 [physics].

³⁸Y.-P. Chang, K. Długołęcki, J. Küpper, D. Rösch, D. Wild, and S. Willitsch, "Specific chemical reactivities of spatially separated 3-aminophenol conformers with cold Ca^+ ions," Science **342**, 98–101 (2013), arXiv:1308.6538 [physics].

³⁹N. Teschmit, D. A. Horke, and J. Küpper, "Spatially separating the conformers of a dipeptide," Angew. Chem. Int. Ed. **57**, 13775–13779 (2018), arXiv:1805.12396 [physics].

⁴⁰J. Onvlee, S. Trippel, and J. Küpper, "Ultrafast light-induced dynamics in solvated biomolecules: The indole chromophore with water," Nat. Commun. **13**, 7462 (2022), arXiv:2103.07171 [physics].

⁴¹H. Stapelfeldt and T. Seideman, "Colloquium: Aligning molecules with strong laser pulses," Rev. Mod. Phys. **75**, 543–557 (2003).

⁴²L. Holmegaard, J. H. Nielsen, I. Nevo, H. Stapelfeldt, F. Filsinger, J. Küpper, and G. Meijer, "Laser-induced alignment and orientation of quantum-state-selected large molecules," Phys. Rev. Lett. **102**, 023001 (2009), arXiv:0810.2307 [physics].

⁴³O. Ghafur, A. Rouzée, A. Gijsbertsen, W. K. Siu, S. Stolte, and M. J. J. Vrakking, "Impulsive orientation and alignment of quantum-state-selected NO molecules," Nat. Phys. **5**, 289–293 (2009).

⁴⁴T. Mullins, E. T. Karamatskos, J. Wiese, J. Onvlee, A. Rouzée, A. Yachmenev, S. Trippel, and J. Küpper, "Picosecond pulse-shaping for strong three-dimensional field-free alignment of generic asymmetric-top molecules," Nat. Commun. **13**, 1431 (2022), arXiv:2009.08157 [physics].

⁴⁵S. Trippel, J. Wiese, T. Mullins, and J. Küpper, "Communication: Strong laser alignment of solvent-solute aggregates in the gas-phase," J. Chem. Phys. **148**, 101103 (2018), arXiv:1801.08789 [physics].

⁴⁶J. C. H. Spence and R. B. Doak, "Single molecule diffraction," Phys. Rev. Lett. **92**, 198102 (2004).

⁴⁷C. J. Hensley, J. Yang, and M. Centurion, "Imaging of isolated molecules with ultrafast electron pulses," Phys. Rev. Lett. **109**, 133202 (2012).

⁴⁸J. Küpper, S. Stern, L. Holmegaard, F. Filsinger, A. Rouzée, A. Rudenko, P. Johnsson, A. V. Martin, M. Adolph, A. Aquila, S. Bajt, A. Barty, C. Bostedt, J. Bozek, C. Caleman, R. Coffee, N. Coppola, T. Delmas, S. Epp, B. Erk, L. Foucar, T. Gorkhover, L. Gumprecht, A. Hartmann, R. Hartmann, G. Hauser, P. Holl, A. Hörmke, N. Kimmel, F. Krasniqi, K.-U. Kühnel, J. Maurer, M. Messerschmidt, R. Moshammer, C. Reich, B. Rudek, R. Santra, I. Schlichting, C. Schmidt, S. Schorb, J. Schulz, H. Soltau, J. C. H. Spence, D. Starodub, L. Strüder, J. Thøgersen, M. J. J. Vrakking, G. Weidenspointner, T. A. White, C. Wunderer, G. Meijer, J. Ullrich, H. Stapelfeldt, D. Rolles, and H. N. Chapman, "X-ray diffraction from isolated and strongly aligned gas-phase molecules with a free-electron laser," Phys. Rev. Lett. **112**, 083002 (2014), arXiv:1307.4577 [physics].

⁴⁹A. Barty, J. Küpper, and H. N. Chapman, "Molecular imaging using x-ray free-electron lasers," Annu. Rev. Phys. Chem. **64**, 415–435 (2013).

⁵⁰M. Zhang, S. Zhang, Y. Xiong, H. Zhang, A. A. Ischenko, O. Vendrell, X. Dong, X. Mu, M. Centurion, H. Xu, R. J. D. Miller, and Z. Li, "Quantum state tomography of molecules by ultrafast diffraction," Nat. Commun. **12**, 5441 (2021).

⁵¹M. Centurion, T. J. Wolf, and J. Yang, "Ultrafast imaging of molecules with electron diffraction," Annu. Rev. Phys. Chem. **73**, 21–42 (2022).

⁵²M. Beye, M. Gühr, I. Hartl, E. Plönjes, L. Schaper, S. Schreiber, K. Tiedtke, and R. Treusch, "FLASH and the FLASH2020+ project – current status and upgrades for the free-electron laser in Hamburg at DESY," Eur. Phys. J. Plus **138**, 193 (2023).

⁵³P. Abbamonte, F. Abild-Pedersen, P. Adams, M. Ahmed, F. Albert, R. Mori, P. Anfinrud, A. Aquila, M. Armstrong, J. Arthur, J. Bargat, A. Barty, U. Bergmann, N. Berrah, G. Blaj, H. Bluhm, C. Bolme, C. Bostedt, S. Boutet, G. Brown, P. Bucksbaum, M. Cargnello, G. Carini, A. Cavalleri, V. Cherezov, W. Chiu, Y. Chuang, D. Cocco, R. Coffee, G. Collins, A. Cordones-Hahn, J. Cryan, G. Dakovski, M. Dantus, H. Demirci, P. Denes, T. Devreux, Y. Ding, S. Doniach, R. Dorner, M. Dunne, H. Durr, T. Egami, D. Eisenberg, P. Emma, C. Fadley, R. Falcone, Y. Feng, P. Fischer, F. Fiuzza, L. Fletcher, L. Foucar, M. Frank, J. Fraser, H. Frei, D. Fritz, P. Fromme, A. Fry, M. Fuchs, P. Fuoss, K. Gaffney, E. Gamboa, O. Gessner, S. Ghimire, A. Gleason, S. Glenzer, T. Gorkhover, A. Gray, M. Guehr, J. Guo, J. Hajdu, S. Hansen, P. Hart, M. Hashimoto, J. Hastings, D. Haxton, P. Heimann, T. Heinze, A. Hexemer, J. Hill, F. Himpsel, P. Ho, B. Hogue, Z. Huang, M. Hunter, G. Hura, N. Huse, Z. Hussain, M. Ilchen, C. Jacobsen, C. Kenney, J. Kern, S. Kevan, J. Kim, H. Kim, P. Kirchmann, R. Kirian, S. Kivelson, C. Kliewer, J. Koral, G. Kovacs, A. Lanzara, J. LaRue, H. Lee, J. Lee, W. Lee, Y. Lee, I. Lindau, A. Lindenberger, Z. Liu, D. Lu, U. Lundstrom, A. MacDowell, W. Mao, J. Marangos, G. Marcus, T. Martinez, W. McCurdy, G. McDermott, C. McGuffey, M. Minitti, S. Miyabe, S. Moeller, R. Moore, S. Mukamel, K. Nass, A. Natan, K. Nelson, S. Nemšák, D. Neumark, R. Neutze, A. Nilsson, D. Nordlund, J. Norskov, S. Nozawa, H. Ogasawara, H. Ohldag, A. Orville, D. Osborn, T. Osipov, A. Ourmazd, D. Parkinson, C. Pellegrini,

- G. Phillips, T. Rasing, T. Raubenheimer, T. Recigno, A. Reid, D. Reis, A. Robert, J. Robinson, D. Rolles, J. Rost, S. Roy, A. Rudenko, T. Russell, R. Sandberg, A. Sandhu, N. Sauter, I. Schlichting, R. Schlogl, W. Schlotter, M. Schmidt, J. Schneider, R. Schoenlein, M. Schoeffler, A. Scholl, Z. Shen, O. Shpyrko, T. Silva, S. Sinha, D. Slaughter, J. Sobota, D. Sokaras, K. Sokolowski-Tinten, S. Southworth, J. Spence, C. Stan, J. Stohr, R. Stroud, V. Sundstrom, C. Taatjes, A. Thomas, M. Trigo, Y. Tsui, J. Turner, A. v. Buuren, S. Vinko, S. Wakatsuki, J. Wark, P. Weber, T. Weber, M. Wei, T. Weiss, P. Wernet, W. White, P. Willmott, K. Wilson, W. Wurth, V. Yachandra, J. Yano, D. Yarotski, L. Young, Y. Zhu, D. Zhu, and P. Zwart, "New science opportunities enabled by LCLS-II x-ray lasers," *Tech. Rep. SLAC-R-1053* (SLAC National Accelerator Laboratory, Menlo Park, CA, USA, 2015).
- ⁵⁴J. S. Kienitz, K. Dlugolecki, S. Trippel, and J. Küpper, "Improved spatial separation of neutral molecules," *J. Chem. Phys.* **147**, 024304 (2017), arXiv:1704.08912 [physics].
- ⁵⁵U. Even, "The Even-Lavie valve as a source for high intensity supersonic beam," *Eur. Phys. J. Techn. Instrumen.* **2**, 17 (2015).
- ⁵⁶F. Filsinger, J. Küpper, G. Meijer, L. Holmegaard, J. H. Nielsen, I. Nevo, J. L. Hansen, and H. Stapelfeldt, "Quantum-state selection, alignment, and orientation of large molecules using static electric and laser fields," *J. Chem. Phys.* **131**, 064309 (2009), arXiv:0903.5413 [physics].
- ⁵⁷T. Tschentscher, C. Bressler, J. Grünert, A. Madsen, A. P. Mancuso, M. Meyer, A. Scherz, H. Sinn, and U. Zastrau, "Photon beam transport and scientific instruments at the European XFEL," *Appl. Sci.* **7**, 592 (2017).
- ⁵⁸M. Johny, J. Onytle, T. Kierspel, H. Bieker, S. Trippel, and J. Küpper, "Spatial separation of pyrrole and pyrrole-water clusters," *Chem. Phys. Lett.* **721**, 149–152 (2019), arXiv:1901.05267 [physics].
- ⁵⁹C. Eon, C. Pommier, and G. Guiochon, "Vapor pressures and second virial coefficients of some five-membered heterocyclic derivatives," *J. Chem. Eng. Data* **16**, 408–410 (1971).
- ⁶⁰W. Christen, "Stationary flow conditions in pulsed supersonic beams," *J. Chem. Phys.* **139**, 154202 (2013).
- ⁶¹Y.-P. Chang, F. Filsinger, B. Sartakov, and J. Küpper, "CMIs-TARK: Python package for the Stark-effect calculation and symmetry classification of linear, symmetric and asymmetric top wavefunctions in dc electric fields," *Comp. Phys. Comm.* **185**, 339–349 (2014), current version available from GitHub, arXiv:1308.4076 [physics].
- ⁶²M. Johny, C. A. Schouder, A. Al-Refaie, L. He, J. Wiese, H. Stapelfeldt, S. Trippel, and J. Küpper, "Water is a radiation protection agent for ionised pyrrole," *Phys. Chem. Chem. Phys.* **26**, 13118–13130 (2024), arXiv:2010.00453 [physics].
- ⁶³S. Hankin, D. Villeneuve, P. Corkum, and D. Rayner, "Intense-field laser ionization rates in atoms and molecules," *Phys. Rev. A* **64**, 013405 (2001).
- ⁶⁴J. Wiese, J.-F. Olivieri, A. Trabattoni, S. Trippel, and J. Küpper, "Strong-field photoelectron momentum imaging of OCS at finely resolved incident intensities," *New J. Phys.* **21**, 083011 (2019), arXiv:1904.07519 [physics].
- ⁶⁵K. Fehre, D. Trojanowskaja, J. Gatzke, M. Kunitski, F. Trinter, S. Zeller, L. P. H. Schmidt, J. Stohner, R. Berger, A. Czasch, O. Jagutzki, T. Jahnke, R. Dörner, and M. S. Schöffler, "Absolute ion detection efficiencies of microchannel plates and funnel microchannel plates for multi-coincidence detection," *Rev. Sci. Instrum.* **89**, 045112 (2018).
- ⁶⁶S. Trippel, Y.-P. Chang, S. Stern, T. Mullins, L. Holmegaard, and J. Küpper, "Spatial separation of state- and size-selected neutral clusters," *Phys. Rev. A* **86**, 033202 (2012), arXiv:1208.4935 [physics].
- ⁶⁷L. Holmegaard, J. L. Hansen, L. Kalhøj, S. L. Krøgh, H. Stapelfeldt, F. Filsinger, J. Küpper, G. Meijer, D. Dimitrovski, M. Abu-samha, C. P. J. Martiny, and L. B. Madsen, "Photoelectron angular distributions from strong-field ionization of oriented molecules," *Nat. Phys.* **6**, 428 (2010), arXiv:1003.4634 [physics].